

# Probability distribution method based on the triple porosity model to identify the fluid properties of the volcanic reservoir in the Wangfu fault depression by well log

Lihua Zhang<sup>1</sup> · Baozhi Pan<sup>1</sup> · Gangyi Shan<sup>1</sup> · Sihui Liu<sup>1</sup> ·  
Yuhang Guo<sup>1</sup> · Chunhui Fang<sup>1</sup>

Received: 8 November 2015 / Accepted: 1 December 2016 / Published online: 28 December 2016  
© Springer International Publishing Switzerland 2016

**Abstract** Due to the powerful anisotropy of the physical properties of volcanic reservoirs, their component minerals and pore configuration are very complex, rendering fluid identification very difficult. This paper first computed the cementation exponent, which was based on triple porosity model, then used the varied matrix density and matrix neutron to compute the porosity, and finally combined with resistivity well log, and a  $P^{1/2}$  probability distribution curve was built. The fluid properties were predicted from the shape of the  $P^{1/2}$  probability distribution curve. Good results were achieved when these methods were used in the volcanic reservoir of the Wangfu fault depression, which indicated that these methods can be used in the fluid property identification of volcanic reservoirs and can also be referred to for other lithology reservoirs.

**Keywords** Volcanic reservoir · Fluid identification · Varied matrix · Probability distribution · Triple porosity model

## 1 Introduction

In the past several years, along with the development of petroleum prospecting and exploration technology, the positions of lithology and lowporosity and lowpermeability reservoirs have become increasingly important. The fluid property identification of complicated reservoirs has

attracted increasingly great concern. Many researchers are currently studying fluid identification methods. Zhang et al. [1] used compressional wave and transversal wave data to predict the fluid properties of volcanic reservoirs in the Changling area. Liang and Wang [2] associated well log with mud logging to discriminate gas and water pay. Li [3] used electric imaging and nuclear magnetic resonance to identify fluid typing for complex reservoirs. Combining statistics theory, Gui et al. [4] optimized fluid factors which are not affected by background lithology and fluid-type numbers to identify fluids. Sui et al. [5] used the work index ratio to fracture interpretation and evaluation and fluid identification for igneous rock reservoirs in the Zhongguai area, Xinjiang. Fan et al. [6] used the Fisher discriminant analysis to identify fluids in a tight sandstone reservoir in the Xujiahe Formation, northeastern Sichuan Basin.

We can see that there are many methods for identifying fluid properties, but methods which are fit for volcanic reservoirs are few in number. For this type reservoir, resistivity and sonic log responding to gas and water pay are simultaneously affected by many elements, such as lithology and pore configuration. The log response characteristics are not obvious; thus mathematical approaches are needed for conventional well logs to research the methods of identifying the gas and water pay.

The Wangfu fault depression is situated in the southeast uplifted area of the Songliao Basin. The lithology in the Huoshiling Formation is mainly intermediate volcanic rock [7], including andesite, trachyte, and little tuff (breccia) molten lava, and is very complicated. Moreover, the reservoir space types and their assemblage characters of different lithologies are different. The main space types include inter-granular pore, dissolution pore, inner pore, and structural fracture. The types of space combination of volcanic lava reservoirs are almond in the pores, solution pores

---

✉ Gangyi Shan  
shangangyi@jlu.edu.cn

<sup>1</sup> College of Geo-Exploration Science and Technology,  
Jilin University, Changchun 130026, China

and fracture type, while the types of the space combination of pyroclastic rock reservoirs are inter-granular pore and dissolved pore and the structural fractures are developed in all volcanic rocks. All of these increase the difficulty of fluid property identification. According to the pore characters and conductive mechanisms, this paper used the triple porosity model to compute the cementation exponent and a neutron-density cross plot to compute the total porosity after continuously varied matrix neutron and density were achieved from elemental capture spectroscopy (ECS). The probability distribution  $P^{1/2}$  was built to identify the fluid property combining cementation exponent and total porosity with resistivity log curve.

### 2 Pore characters of volcanic rock and triple porosity model

The pore configuration of volcanic rock is very complicated, such as primary air hole, residual air hole, pore among phenocrysts, pore in almond corpus, corrosion pore, dissolved pore, and inter-granular pore. Moreover, structural or dissolved fractures are developed in volcanic rock. Figure 1 shows the statistical graph of every pore character of the 58 casting slices in five wells and shows that the pore configuration is very complicated. Complicated pore configuration results in complicated conductive mechanisms.

Aguilera and Aguilera [8] proposed a triple porosity model, which was composed of non-connected pores, fractures and matrix pores. His model considered four types of porosity. The first is matrix porosity, which is equal to void space in the matrix divided by the bulk volume of the matrix system. The second is also matrix porosity, which is equal to the void space in the matrix divided by the bulk volume of the triple porosity system. The third is fracture porosity, which is equal to the void space of the fractures divided by the bulk volume of the triple porosity system. The fourth is the porosity of the non-connected vugs, which

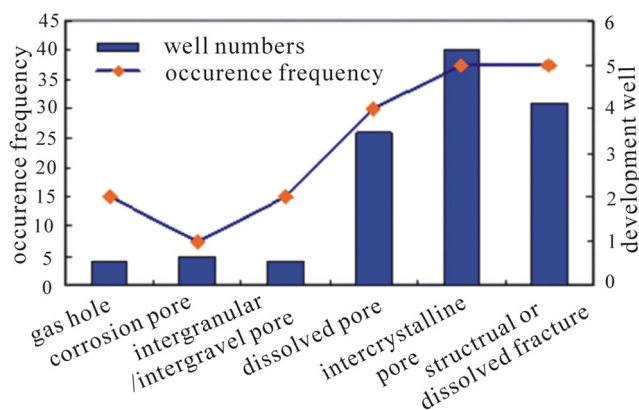


Fig. 1 Statistical graph of each pore character

is equal to the void space of the non-connected vugs divided by the bulk volume of the triple porosity system. The triple porosity system is also referred to as the composite system. A triple porosity reservoir can be modeled as a parallel resistance network for the matrix and fractures, and a series resistance network for the non-connected vugs and the matrix/fractures combination. Zhang et al. [9] applied this model to the volcanic reservoir in the deep northern Songliao Basin, and good results were achieved. Based on this model, the following formula can be derived, which was used to compute the cementation exponent  $m$ :

$$m = \frac{-\log \left[ \phi_{nc} + \frac{(1-\phi_{nc})}{\phi_2 + (1-\phi_2)/\phi_b^{-m_b}} \right]}{\log \phi} \tag{1}$$

In this paper research, the cementation exponent  $m$  was computed from the above formula, where  $m$  is dimensionless. In Eq. 1,  $\phi$  is the total porosity;  $\phi_b$  is the matrix block porosity attached to the bulk volume of the matrix system;  $\phi_{nc}$  is the porosity of the non-connected vug attached to the bulk volume of the composite system;  $\phi_2$  is the porosity of the natural fractures attached to the bulk volume of the composite system, where the units of all porosities are fractions; and  $m_b$  is the cementation exponent of the matrix which was determined from the analysis of the unfractured and non-vuggy plugs, where the units of all porosities are dimensionless.

Due to the component complexity of volcanic rocks, even if they bear the same lithologies, they may still have different matrix parameters. The matrix parameters were confirmed by statistical analysis methods in previous research. Moreover, single defined matrix parameters were used in single well processing, which was not in accordance with the characters of complicated lithology. In the present study,

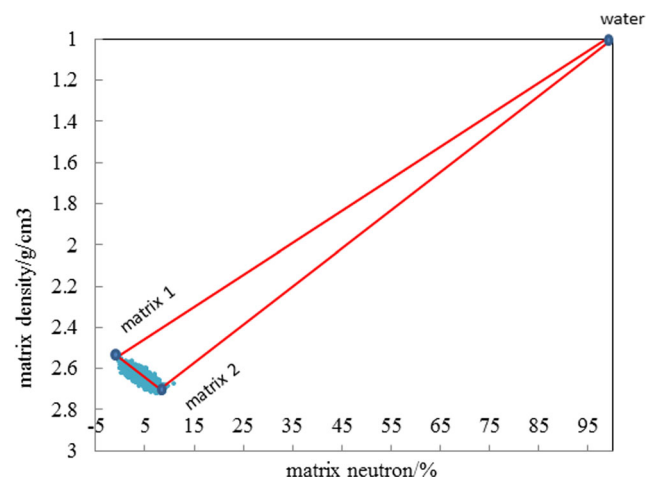


Fig. 2 Cross plot of matrix neutron and matrix density

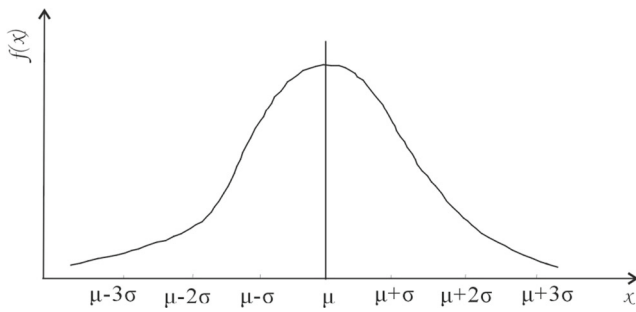


Fig. 3 Normal distribution diagram

ECS log data were sufficiently used, and varied matrix neutron and varied matrix density parameters were computed by means of multi-parameter assemblage. The computation formula of varied matrix density is as follows [10]:

$$\rho_{ma} = 3.1475 - 1.1003 \times W_{Si} - 0.9834 \times W_{Ca} - 2.4385 \times W_{Na} - 2.4082 \times W_K + 1.4245 \times W_{Fe} - 11.31 \times W_{Ti} \quad (2)$$

The computation formula of the varied matrix neutron is as follows [9]:

$$\phi_{Nma} = 0.3517 - 0.728 \times W_{Si} - 0.7579 \times W_{Ca} - 1.5533 \times W_{Na} - 1.0979 \times W_K - 0.2408 \times W_{Fe} + 9.3709 \times W_{Ti} \quad (3)$$

In the above formula,  $\rho_{ma}$  is the matrix density ( $g/cm^3$ )  $\phi_{Nma}$  is the matrix neutron (%) and  $W_{Si}$ ,  $W_{Ca}$ ,  $W_{Na}$ ,  $W_K$ ,  $W_{Fe}$ , and  $W_{Ti}$  are the respective weight percentage contents of silicon, calcium, sodium, potassium, iron, and titanium elements, which were achieved from the ECS well log (%).

After the matrix neutron and matrix density were determined, the total porosity of volcanic rock could be computed using the neutron-density crossplot method, similar to sand and shale reservoirs. Figure 2 shows the cross plot of the matrix neutron and matrix density. In Fig. 1, the data are derived from the above formula, and matrix 1 and matrix 2 are the average values of the data points on either end.

The fracture porosity was computed from the deep and shallow dual lateral resistivity using the following formula:

$$\phi_2 = m_f \sqrt{R_{mf} \left( \frac{1}{R_s} - \frac{1}{R_d} \right)} \quad (4)$$

where  $R_d$  and  $R_s$  are the deep and shallow dual lateral resistivity ( $\Omega \cdot m$ ) respectively;  $R_{mf}$  is the mud filtrate resistivity ( $\Omega \cdot m$ ); and  $m_f$  is the cementation exponent of the fracture, which is dimensionless.

In view of the complexity of the mineral components of volcanic rock, the difference between the matrix acoustic travel time of different lithologies is very large; thus single matrix acoustic travel time cannot be used in the way that it can for sand and shale profiles. In the present paper, multivariate regression was used to achieve varied composite matrix acoustic travel time, and the formula for which is as follows:

$$\Delta t_{ma} = 104.0562 - 119.7988 \times W_{Si} + 174.3562 \times W_{Ca} + 332.4925 \times W_{Na} + 233.1537 \times W_K - 204.073 \times W_{Fe} + 2631.707 \times W_{Ti} \quad (5)$$

Next, the matrix porosity was computed by means of the Wyllie equation

$$\phi_m = \frac{\Delta t - \Delta t_{ma}}{\Delta t_f - \Delta t_{ma}} \quad (6)$$

Fig. 4 Porosity and cementation exponent synthetic graphs of wells A and B

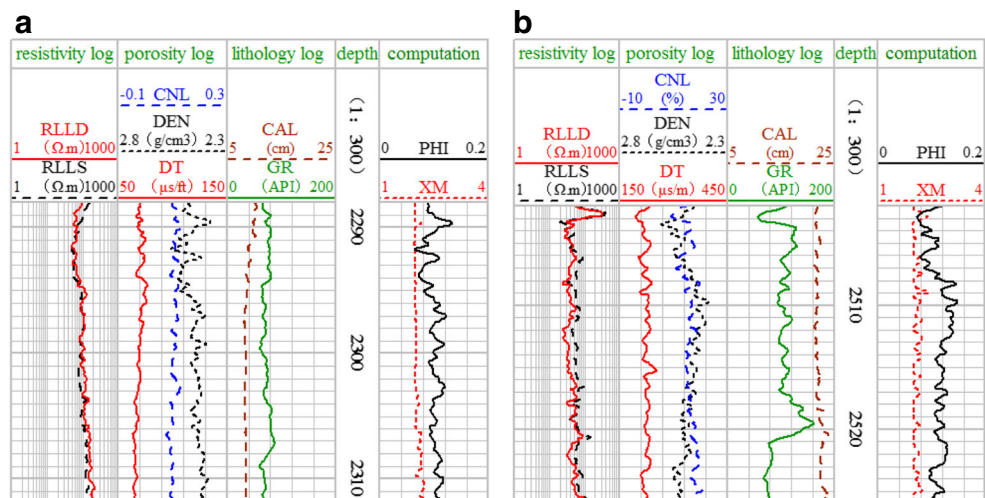
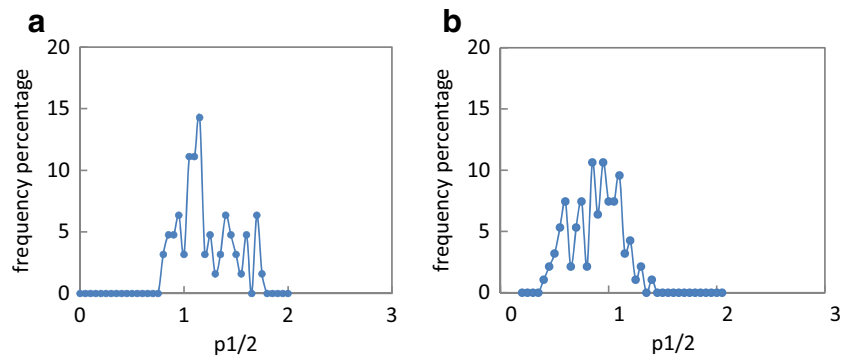


**Fig. 5** Probability distribution diagrams of gas-bearing intervals of wells A and B



where  $\Delta t$  is the acoustic travel time well log and  $\Delta t_f$  is the acoustic travel time of the fluid, where the units of  $\Delta t$ ,  $\Delta t_f$ , and  $\Delta t_{ma}$  are microseconds per meter.

### 3 $P^{1/2}$ probability distribution method

Normal distribution was first proposed by De Moivre in a book in 1718, followed by a paper regarding binomial distribution in 1734. When the position parameter  $n$  of the random binomial variable is very large and the shape parameter  $P$  is equal to  $1/2$ , the approximate distribution function of the binomial distribution which was derived is called normal distribution. Normal distribution is a convenient model for quantity phenomena in natural science and behavior science. Many types of psychological tests and physical phenomena approximately obey normal distribution. If many small actions are added as a variable, then this variable follows normal distribution, and this can be confirmed theoretically [11].

In probability theory, normal distribution is the limit distribution of some continuous and discrete distributions. If

random variable  $X$  obeys a probability distribution whose position parameter is  $\mu$  the dimension parameter is  $\sigma$  and  $X$  is signed as  $X \sim N(\mu, \sigma^2)$ , and then its probability density function is  $f(x) = \frac{1}{\sigma\sqrt{2\pi}} e^{-\frac{(x-\mu)^2}{2\sigma^2}}$ , and the mathematical expectation or expectation value  $\mu$  of the distribution is equal to the position parameter, which determines the position of distribution; finally, variance  $\sigma^2$  or standard difference  $\sigma$  is equal to the dimension parameter, which determines the amplitude of distribution (see Fig. 3).

The apparent formation water resistivity  $R_{wa} = R_t \times \phi^m$  is derived from the Archie equation  $F = \frac{R_0}{R_w}$ . By contrasting  $R_{wa}$  with  $R_w$ , which is the formation of water resistivity, the fluid properties of the reservoir are discriminated. However, due to the fact that the values of  $R_w$ ,  $\phi$  and  $m$  cannot be accurately obtained, the error rate of the computed  $R_{wa}$  is very high, which makes it very difficult to identify the fluid properties by using it. Therefore, we adopted a special mathematical method, i.e. the normal distribution method, to denote the fluid properties of the reservoir. That is to say, the alternation pattern of  $R_{wa}$ , not the absolute value of  $R_{wa}$ ,

**Fig. 6** Porosity and cementation exponent synthetic graphs of wells C and D

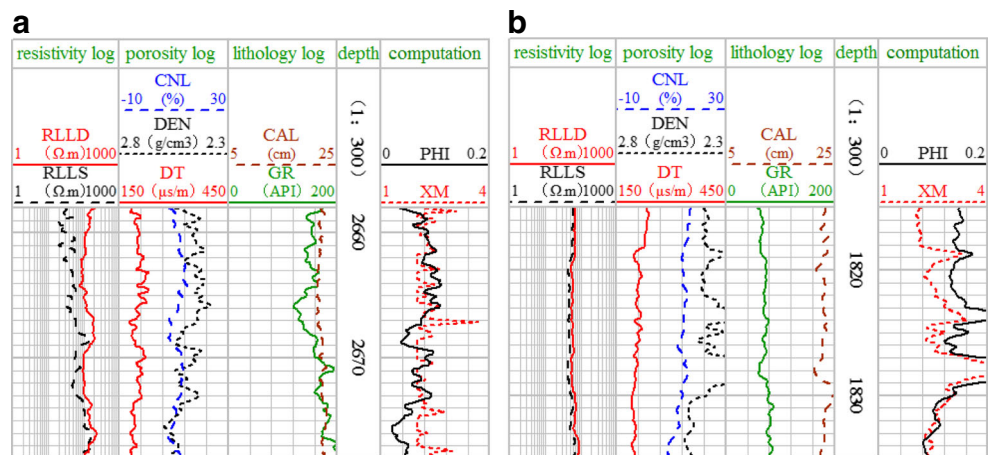
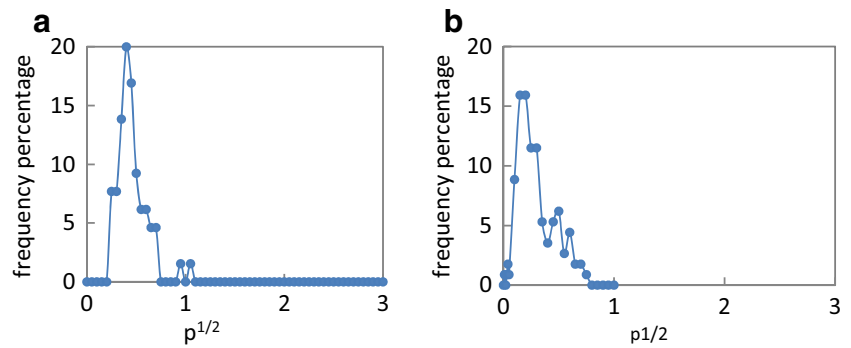


**Fig. 7** Probability distribution diagrams of gas-bearing intervals of wells C and D



was used to denote the fluid property of the reservoir. The square root of  $R_{wa}$  is extracted and is referred to as  $P^{1/2}$

$$P^{1/2} = (R_{wa})^{\frac{1}{2}} = (R_t \times \phi^m)^{\frac{1}{2}} \tag{7}$$

In Eq. 7,  $\phi$  is the total porosity which is computed from the above neutron-density cross plot,  $R_t$  is the resistivity curve from the well log, and  $m$  is the cementation exponent which is computed from Eq. 1. The  $P^{1/2}$  values of the measuring points in some intervals are in accordance with the normal distribution pattern. The size of  $\sigma$  reflects the divergence degree of the normal curve; i.e. the more divergent the value of the measuring point, the greater are the values of  $\sigma$ .

### 4 Applications

The research methods described above were applied to the medium volcanic rock of the Huoshiling formation in the Wangfu fault depression to identify its fluid properties. Forty-one internals of 11 wells were processed. The following are the four intervals of four wells. In the following diagrams, PHI is the total porosity, which was computed by the neutron-density cross plot, and XM is the cementation exponent, which was computed by the above formula. Figure 4 shows the well logs, computed total porosity and cementation exponent synthetic diagrams of wells A and B. Figure 5 shows the  $P^{1/2}$  probability distribution diagrams of the gas layers in wells A and B. On the basis of the probability distribution curves, these curves are relatively smooth and fat. Gas testing was performed at the interval of 2295.5–2303.3 m in well A, with a daily gas yield of 73.89 kg/m<sup>3</sup>, and the test result is gas pay. The interval of 2506–2517.6 m in well B also shows gas testing, with a daily gas yield of 154.79 kg/m<sup>3</sup>, and the test result is gas pay.

Figure 6 shows the well logs, computed total porosity and cementation exponent synthetic diagrams of wells C and D. Figure 7 shows the  $P^{1/2}$  probability distribution diagrams of the water layers in wells C and D. On the

basis of the probability distribution curves, these curves are relatively steep and thin. Gas testing was performed at the interval of 1818–1826 m in well C, with a daily water yield of 80.48 m<sup>3</sup>, and the test result is water pay. The interval of 2661–2675 m in well D also shows gas testing, with a daily water yield of 62.9 m<sup>3</sup>, and the test result is water pay.

Generally speaking, in the water pay, the  $\sigma$  is small, and the probability distribution curve is relatively steep and thin, while in the gas pay, the  $\sigma$  is large, and the probability distribution curve is relatively smooth and fat.

### 5 Conclusions

In the present paper, the cementation exponent was computed by the formula derived from the triple porosity model, on the basis of which the matrix and fracture were modeled as a parallel resistance network, and then the matrix/fracture combination and non-connected vugs were modeled as a series resistance network. After the continuously varied matrix neutron and matrix density were determined from the element capture spectroscopy log, the neutron-density cross plot was used to compute the total porosity. Finally, the  $P^{1/2}$  was built by combining the cementation exponent, total porosity, and resistivity curve. The triple porosity model is shown to be suitable for the petrophysical evaluation of volcanic reservoirs which are composed mainly of a matrix, fractures, and non-connected vugs. The alternation pattern of  $R_{wa}$ , not the absolute value of  $R_{wa}$ , was used to denote the fluid properties of the reservoir. Generally speaking, in the water pay, the probability distribution curve was relatively steep and thin, while in the gas pay, the probability distribution curve was relatively smooth and fat. The interpretative results and testing results, through actual data processing, are shown to be in accordance. The research methods described above can be applied to identify the fluid properties of volcanic rock and can also identify the direct fluid properties of other lithology reservoirs.

**Acknowledgments** We warmly acknowledge the financial support from the National Natural Science Foundation of China (Grant No. 41174096). We are also grateful to the anonymous referees for their constructive comments and suggestions.

## References

1. Zhang, L.H., Pan, B.Z., Shan, G.Y.: Fluid property logging prediction of volcanic reservoirs in the Changling area. *Prog. Geophys.* (in Chinese) **24**(6), 2151–2155 (2009)
2. Liang, C.J., Wang, B.Q.: Exactly deciding hydrocarbon reservoir through combining well logs with geological log data. *Nat. Gas Ind.* **23**(S1), 52–56 (2004)
3. Li, Z.B.: Problem and advance on the fluid typing for complex reservoirs using well log. *Oil Gas Geol.* **25**(4), 356–362 (2004)
4. Gui, J.Y., Gao, J.H., Li, S.J., et al.: Reservoir-oriented fluid factor optimization method. *OGP* **50**(1), 129–135 (2015)
5. Sui, Z.D., Hu, Z.M., Qin, B.J., et al.: Fracture interpretation and evaluation and fluid identification with mud logging work index ratio for igneous rock reservoirs in Zhongguai area, Xinjiang. *Mud Logging Engineering* **26**(1), 13–17 (2015)
6. Fan, R., Zhou, L., Wu, J., et al.: Research on tight sandstone reservoir fluids identification in Xujiache Formation, northeastern Sichuan basin. *Petroleum Geology and Recovery Efficiency* **22**(3), 67–71 (2015)
7. Sun, H.B.: Volcanic Reservoir Characteristics and Distribution in Wangfu Fault Depression of Southern Songliao Basin. Jilin University, Changchun (2014)
8. Aguilera, R.F., Aguilera, R.: A triple porosity model for petrophysical analysis of naturally fractured reservoirs. *Petrophysics* **45**(2), 157–166 (2004)
9. Zhang, L.H., Pan, B.Z., Shan, G.Y.: Tri-porosity model and its application in igneous reservoir. *Well Logging Technology* **32**(1), 37–40 (2008)
10. Feng, Q.F.: Study of Logging Interpretation Method for Deep Igneous Rock Gas Reservoir in Daqing Xujiaweizi area. Qingdao Ocean University of China (2007)
11. Xiao, Y.N., Ru, S.C., Ouyang, K.Z., et al.: Newly Edited Probability Theory and Mathematical Statistics. Beijing University Press, Beijing (2013)